Laboratory experiments on CO2 gas exchange with wave breaking

shuo li[1], Alexander V. Babanin[2], Fangli Qiao[3], Dejun Dai[4], Shumin Jiang[5], and Changlong Guan[6]

[1]University of Melbourne
[2]Department of Infrastructure Engineering, University of Melbourne
[3]First Institute of Oceanography, Ministry of Natural Resources
[4]The First Institute of Oceanography
[5]First Institute of Oceanography
[6]Ocean University of China

November 23, 2022

Abstract

The 2 gas transfer velocity (2) at air-sea interface is usually parameterized with the wind speed, but to a great extent is defined by waves and wave breaking. To investigate the direct relationship between 2 and waves, laboratory experiments are conducted in a wind-wave flume. Three kind of waves are forced in the flume: monochromatic waves generated by a wavemaker, mechanically-generated monochromatic waves with superimposed wind forcing, and pure wind waves with 10-meter wind speed ranging from 4.5 m/s to 15.5 m/s. The wave parameters are found to be well correlated with 2 while wind speed alone can not adequately describe 2 . To reconcile the data sets, non-dimensional empirical formulae are established in which 2 is expressed as a function of wave parameters as the dominant term and an enhancement factor to account for additional influence of the wind.

Laboratory experiments on CO_2 gas exchange with wave breaking

Shuo Li[1], Alexander V. Babanin[1,2], Fangli Qiao[2,3]Dejun Dai[3], Shumin Jiang[3], Changlong Guan[4]

[1]Department of infrastructure Engineering, University of Melbourne, Melbourne, Victoria, Australia

[2]Laboratory for Regional Oceanography and Numerical Modeling, National Laboratory for Marine Science and Technology, Qingdao, 266237, China

[3]First Institute of Oceanography, Ministry of Natural Resources, Qingdao, China

[4]College of Oceanic and Atmospheric Sciences, Ocean University of China, Qingdao, China

Key Points:

- Carbon dioxide gas transfer velocity at air-water interface is measured during wave breaking in laboratory.
- The gas transfer velocity is found to be well correlated with waves and wave breaking.
- Non-dimensional parameterization is established to describe the gas transfer velocity with waves.

Corresponding author: Shuo Li, `leeshuo1991@gmail.com`

Abstract

The CO_2 gas transfer velocity (K_{CO_2}) at air-sea interface is usually parameterized with the wind speed, but to a great extent is defined by waves and wave breaking. To investigate the direct relationship between K_{CO_2} and waves, laboratory experiments are conducted in a wind-wave flume. Three kind of waves are forced in the flume: monochromatic waves generated by a wavemaker, mechanically-generated monochromatic waves with superimposed wind forcing, and pure wind waves with 10-meter wind speed ranging from 4.5 m/s to 15.5 m/s. The wave parameters are found to be well correlated with K_{CO_2} while wind speed alone can not adequately describe K_{CO_2}. To reconcile the data sets, non-dimensional empirical formulae are established in which K_{CO_2} is expressed as a function of wave parameters as the dominant term and an enhancement factor to account for additional influence of the wind.

Plain Language Summary

The CO_2 gas transfer is usually parameterized in terms of the wind speed, but to a great extent is defined by waves and wave breaking in particular. While wind and waves are connected in general, this connection is very complex. In this paper, the relationship between gas transfer velocity (K_{CO_2}) and wave breaking is investigated. The results show that the wave parameters are well correlated with K_{CO_2} while wind speed alone can not fully describe K_{CO_2}. Therefore, wave properties are considered directly in the parameterization of K_{CO_2}. The empirical formulae are established in which K_{CO_2} is expressed as a function of wave breaking parameters and a scaled factor to account for additional influence of the wind.

1 Introduction

Atmospheric carbon dioxide has been accumulating in the past few decades due to excessive anthropogenic activities and fossil fuel combustion, which exerts impact on global climate change and carbon cycle (Pachauri et al., 2014). The ocean is one of the largest reservoirs for gaseous CO_2 and has the potential to absorb or release CO_2 through gas exchange across air-sea interface. The CO_2 flux (F) between the atmosphere and ocean is generally described as the product of gas transfer velocity (K_{CO_2}), gas solubility (s) in sea water and thermodynamic driving force in terms of partial pressure difference:

$$F = K_{CO_2} \cdot s \cdot (pCO_{2w} - pCO_{2a}), \tag{1}$$

where pCO_{2w} and pCO_{2a} denote the water-side and air-side CO_2 partial pressure, respectively.

The parameterization of gas transfer velocity (K_{CO_2}) has been a major research topic for years. K_{CO_2} is a kinetic function of environmental forcing factors such as wind speed, wave properties and bubble production. Because most of the relevant dynamic processes can scale with wind speed, K_{CO_2} is generally parameterized with the wind speed through a linear, quadratic or cubic relation (Wanninkhof et al., 2009). However, uncertainties in the relationships imply that wind speed alone may not be sufficient to quantify K_{CO_2}. For sparingly soluble gas such as CO_2, K_{CO_2} is regulated by water-side turbulence (Jähne et al., 1987) which is often induced by waves and wave breaking.

The importance of wave breaking on air-sea interaction has been discussed in Melville (1996) and A. Babanin et al. (2011). Due to the lost energy, wave breaking enhances intensity of the under-surface turbulence by up to 3 orders of magnitude, and it produces bubbles and may spend up to 50% of energy loss on work against the buoyancy force acting on these bubbles. Wave growth and ultimately its breaking are connected with the wind, hence there is correlation between gas transfer rate and wind speed, but this is by far not a direct connection because the breaking is nonlinear evolution of waves (or wave

superposition), not the wind (A. Babanin et al., 2011). Therefore, physical models including wave effect explicitly should provide improved flux estimates over limited spatial and temporal scales which depart from the mean behavior of the wind speed formulas, and also offer a way to extend gas transfer estimates to conditions beyond the validity of the wind formulas (e.g. tropical cyclones).

Original gas transfer models with water-side turbulent eddies were proposed by Fortescue and Pearson (1967) and Lamont and Scott (1970). Considering the water surface waves, Jähne et al. (1987) found that the mean square slope of the waves was an appropriate parameter to describe the gas transfer velocity. In addition, the dependence of gas transfer rate on Schmidt Number (Sc), which is the ratio of fluid kinematic viscosity and mass diffusivity, changed from $Sc^{-\frac{2}{3}}$ to $Sc^{-\frac{1}{2}}$ at wavy surface. Zappa et al. (2004) found that the gas transfer velocity scaled well with fractional area coverage of microbreakers in the wave tank in the wind speed range 4.2-9.3 m/s. Zhao et al. (2003) attempted to correlate gas transfer velocity with the sea whitecap coverage by using a wind-sea Reynolds number which represented the turbulence generated by waves. The relationship between gas transfer and wind-sea Reynolds numbers were further evaluated in Brumer et al. (2017). They found that the Reynolds numbers performed well in collapsing ocean data sets. The bubble-mediated gas transfer was also studied (e.g. Woolf, 1997; Fairall et al., 2011; Liang et al., 2013) and generally parameterized with wind speed, but it is obvious that the bubbles (except in hurricane-like condition) are produced by wave breaking rather than by the wind.

In our work, laboratory experiments are conducted on how CO_2 gas exchange varies with wave breaking. Experimental setup is introduced in section 2. The relationship between CO_2 transfer velocity and wind and waves is analyzed in section 3. Further discussions and conclusions are presented in section 4.

2 The Experiments

The facility for experiments is a wind-wave flume, 45 m long, 1.8 m high and 1 m wide available at First Institute of Oceanography in China. The tank is filled with tap water up to 1.2 m. The wind fan is installed above the wave tank with closed air channel. A mechanical wavemaker is located upstream. It is programmable and able to generate regular waves, steep enough to lead to wave breaking. At the downstream end of wave tank, a beach is designed for damping wave energy (more than 95%) to prevent the reflection of waves.

Various sensors were employed along the wave tank to measure physical and chemical variables. Water surface elevation was measured by 4 resistance-type wave gauges (figure 1) at 50 Hz sampling rate located at 6.2 m, 14.0 m, 16.6 m and 18.0 m away from the wavemaker. A vertical array of 5 Pitot tubes was located about 10 cm before wave gauge 3, arranged evenly (5 cm spaced) with the lowest one at about 15 cm above the free water surface. It took 100 milliseconds for the computer to record wind speed at each tube. An acoustic Doppler velocimeter (ADV) was collocated with wave gauge 3 to measure turbulence in the water, although the data is not used in the present work. 50 cm downstream of wave gauge 3, tubing for taking water and air samples in the flume was installed, and further connected to the CO_2 analysis devices. Two thermometers were placed at the rear of wave tank for air and water temperature measurements, respectively. Air conditioners in the lab were always running during experiments so that temperature at different locations of wave tank was almost the same. Outside the wave tank, a Canon digital camera and a video camera were employed to record wave breaking processes. In addition, the water acidity index (pH) and air pressure in the lab were also recorded during the experiments.

Figure 1. Schematic showing the deployment of probes in the wave tank.

The instrument for CO_2 analysis was an Apollo pCO_2 system (model AS-P2 by Apollo SciTech, USA) which incorporated an air-water equilibrator and Picarro G2301 CO_2 analyzer with high precision(< 0.15 ppm and < 0.05 ppm for 5-second and 5-minute measurement, respectively). Water was piped out of tank at a rate of around 2.5 L/min into equilibrator to contact with air stream. After reaching equilibrium, the water was returned to the rear of tank and the equilibrated gas was analyzed by Picarro as pCO_{2w} in equation (1). The multi-position valve on Apollo was set up so that Picarro could analyze equilibrated gas samples and ambient air in lab alternatively. Meanwhile, Apollo was able to collect data of both pCO_{2w} and pCO_{2a} from Picarro. An air dryer was used to remove water vapor from the Picarro sample air stream. Standard gases with CO_2 concentration of 400.0 ppm, 600.7 ppm, 799.2 ppm, and 1000.6 ppm were used to calibrate Picarro analyzer. In the flume, an air/water pCO_2 gradient was created to ensure evasion of CO_2 from water into air for all the experiments.

The experimental parameters are listed in table 1. In A1-A10, wave packets generated by a wavemaker were unstable (Banner et al., 2000) and set to break after passing wave gauge 2. Based on A10, A5 and A9, the same mechanically-generated waves were coupled with different superimposed wind in B1-B6 in order to compare with A cases in terms of wave breaking and resulted gas transfer rate. C1-C6 had the waves produced and forced by wind only. The initial wave signal of mechanical waves in A1-B6 was the combination of a carrier sinusoidal wave with frequency f_0, amplitude a_0, wave number $k_0 = (2\pi f_0)^2/g$, where g is gravitational acceleration, steepness $\varepsilon_0 = a_0 k_0$, and a resonant sideband with frequency f_+, amplitude a_+ (10% to 30% with respect to a_0). The Benjamin-Feir Index (BFI) was used to evaluate the instability of wave trains, as $BFI = \varepsilon_0/(\Delta k/k_0)$, where Δk is the wave number difference between carrier wave and sideband. The wind fan frequency (f_{fan}) in B1-C6 was set up beween 10 Hz to 35 Hz for varied wind forcing. The drag coefficient c_d was computed to be 0.0013 at case C6 with a clear logarithmic wind profile. Because a wind-dependent c_d had very slight influence on the coefficients of final formulae, constant $c_d = 0.0013$ was used here to correct the wind speed to 10-meter reference (U_{10}) and to compute wind friction velocity. The records of wave gauge 3 to 4 were used to recognize the breakers because an evident decrease of the wave height after the breaking was observed. By choosing the breaking events that happened upstream nearest the CO_2 sampling tubing, the mean wave height of the breakers (H_b) measured at wave gauge 3, before the breaking, was used as the proxy of wave height of the breaking onset. Similarly, U_{wb} is the mean orbital velocity of the breakers computed following the linear wave theory. For young wind waves (C1-C6), the breaking events were identified by using the criterion for ultimate steepness ($\varepsilon \leq 0.44$) of individual waves subject to modulational instability (A. V. Babanin et al., 2007, 2010). Breaking probability (b_T) was then estimated based on the proportion of breakers. Sig-

Table 1. Experimental parameters of all cases. A1 to A10 are the monochromatic wave experiments with mechanically-generated waves. B1 to B6 are the coupled wave experiments (superimposed wind with mechanically-generated waves). C1 to C6 represent the wind-wave experiments.

Case No.	f_0 (Hz)	a_0 (m)	ε_0	f_+ (Hz)	a_+ (m)	BFI	f_{fan} (Hz)	U_{10} (m/s)	H_b (m)	U_{wb} (m/s)	b_T	H_s (m)	U_{wm} (m/s)	K_{600} (10^{-6} m/s)
A1	1.2	0.035	0.20	1.32	0.010	0.95	0	0	0.15	0.60	0.092	0.32	0.13	1.065
A2	1.2	0.052	0.30	1.33	0.006	1.36	0	0	0.18	0.70	0.103	0.48	0.19	1.386
A3	1.0	0.050	0.20	1.10	0.024	0.95	0	0	0.25	0.82	0.073	0.40	0.19	1.280
A4	1.3	0.029	0.20	1.43	0.007	0.95	0	0	0.10	0.36	0.101	0.30	0.12	0.748
A5	1.1	0.041	0.20	1.21	0.014	0.95	0	0	0.23	0.81	0.090	0.35	0.16	1.492
A6	0.9	0.061	0.20	1.04	0.035	0.60	0	0	0.30	0.90	0.069	0.43	0.22	1.713
A7	1.1	0.033	0.16	1.24	0.019	0.59	0	0	0.15	0.53	0.111	0.31	0.14	1.206
A8	1.1	0.051	0.25	1.24	0.014	0.94	0	0	0.20	0.72	0.111	0.42	0.19	1.396
A9	1.0	0.055	0.22	1.11	0.023	0.95	0	0	0.24	0.76	0.098	0.42	0.20	1.663
A10	0.9	0.055	0.18	1.02	0.039	0.61	0	0	0.29	0.87	0.120	0.40	0.21	2.946
B1	0.9	0.055	0.18	1.02	0.039	—	25	11.21	0.29	0.85	0.121	0.46	0.24	4.790
B2	0.9	0.055	0.18	1.02	0.039	—	15	6.77	0.28	0.82	0.122	0.42	0.22	1.946
B3	1.1	0.041	0.20	1.21	0.014	—	20	9.14	0.20	0.74	0.087	0.40	0.18	2.997
B4	1.1	0.041	0.20	1.21	0.014	—	30	13.43	0.24	0.88	0.086	0.52	0.22	4.101
B5	1.0	0.055	0.22	1.11	0.023	—	20	8.85	0.26	0.86	0.098	0.46	0.22	3.898
B6	1.0	0.055	0.22	1.11	0.023	—	30	13.43	0.27	0.88	0.096	0.55	0.25	6.974
C1	—	—	—	—	—	—	10	4.46	0.02	0.21	0.239	0.15	0.02	0.092
C2	—	—	—	—	—	—	15	6.88	0.03	0.29	0.371	0.22	0.04	0.280
C3	—	—	—	—	—	—	20	9.19	0.04	0.34	0.488	0.27	0.05	0.670
C4	—	—	—	—	—	—	25	11.12	0.05	0.38	0.559	0.31	0.07	0.999
C5	—	—	—	—	—	—	30	13.25	0.07	0.44	0.665	0.39	0.09	—
C6	—	—	—	—	—	—	35	15.44	0.09	0.51	0.732	0.45	0.12	2.743

nificant wave height H_s and mean orbital velocity U_{wm} of all waves at wave gauge 3 were also computed. Plunging or spilling breakers were found for mechanically-generated waves in A1-B6. For fetch-limited wind waves in C1-C6, the change from small breakers without bubble injection to breakers with bubbles were observed when the wind speed was varied from low to high.

The method to calculate gas transfer rate K_{CO_2}, following Ocampo-Torres et al. (1994), is adopted in our work:

$$\frac{\partial C_g}{\partial t}\frac{V_w}{A} = -K_{CO_2}(C_g - C_a), \tag{2}$$

where C_g and C_a are CO_2 concentration detected by Picarro in equilibrated gas and in air, respectively. Here, V_w and A is the water volume and surface area that are involved with the gas exchange processes. So V_w/A identifies the height of water column, which is related to the depth of turbulent mixing layer. Thomson et al. (2016) suggested that the turbulence could be transported down to wave trough due to orbital motion, and in our work the depth of upper mixed layer is scaled with H_b. The calculated K_{CO_2} is further corrected to 20^oC of fresh water with Schmidt number $Sc_{600} = 600$ in order to eliminate the thermal effect on gas transfer.

$$\frac{K_{CO_2}}{K_{600}} = \left(\frac{Sc_{co_2}}{Sc_{600}}\right)^{-0.5}, \tag{3}$$

where K_{600} represents the corrected transfer velocity in table 1, Sc_{co_2} is the Schmidt number of water in laboratory. The power of Sc is empirically determined to be -0.5 for wavy surface (Jähne et al., 1987).

## 3 New Parameterization for CO_2 Gas Transfer Velocity

Compared with groups of monochromatic wave experiments (A5, A9, A10), H_s and K_{600} in B1-B6 become bigger due to superimposed wind while b_T tends to reduce with coupled wind. Wind forcing can slow down the modulation of unstable waves and decrease the number of breakers (A. V. Babanin et al., 2010; Galchenko et al., 2012). Compared with cases B1-B6, C1-C6 have smaller K_{600} in the circumstance of similar wind speed but different wave states.

In the monochromatic wave experiments (A1-A10), K_{600} dependence on b_T is weak (figure 2(a)), correlation between K_{600} and H_b is better (figure 2(b)), but the correlation coefficient between K_{600} and their product $b_T \cdot H_b$ in figure 2(c) is 98%. K_{600} is also found correlated with U_{wb} ($corr = 71\%$) and again the correlation coefficient is improved to be 90% after multiplying b_T to U_{wb} in figure 2(d). The results can be explained as that b_T determines the frequency of occurrence of the water mixing events by breakers, while higher wave height and greater orbital motion imply more turbulence in breaking events. In figure 2(e), K_{600} is also well correlated with the rate of energy loss (P_b) within experimental periods defined by

$$P_b = \frac{\sum(H_{b1}^2 - H_{b2}^2)}{\Delta t}, \tag{4}$$

where H_{b1} and H_{b2} are the wave height before and after wave breaking measured by wave gauges, Δt is the time length of each experiment. P_b contains the information of wave breaking probability and average breaking strength. The energy loss due to breaking is passed to the turbulence whose production rate should be relevant to $b_T \cdot H_b$ and $b_T \cdot U_{wb}$. The results of experiments A1 to A10 demonstrate that wave breaking can still enhance CO_2 gas flux without wind, and wave properties are directly relevant to the CO_2 gas transfer rate.

In coupled wave experiments (B1-B6), CO_2 gas transfer velocity shows good correlation with significant wave height (figure 2(f)), mean wave orbital velocity (figure 2(g))
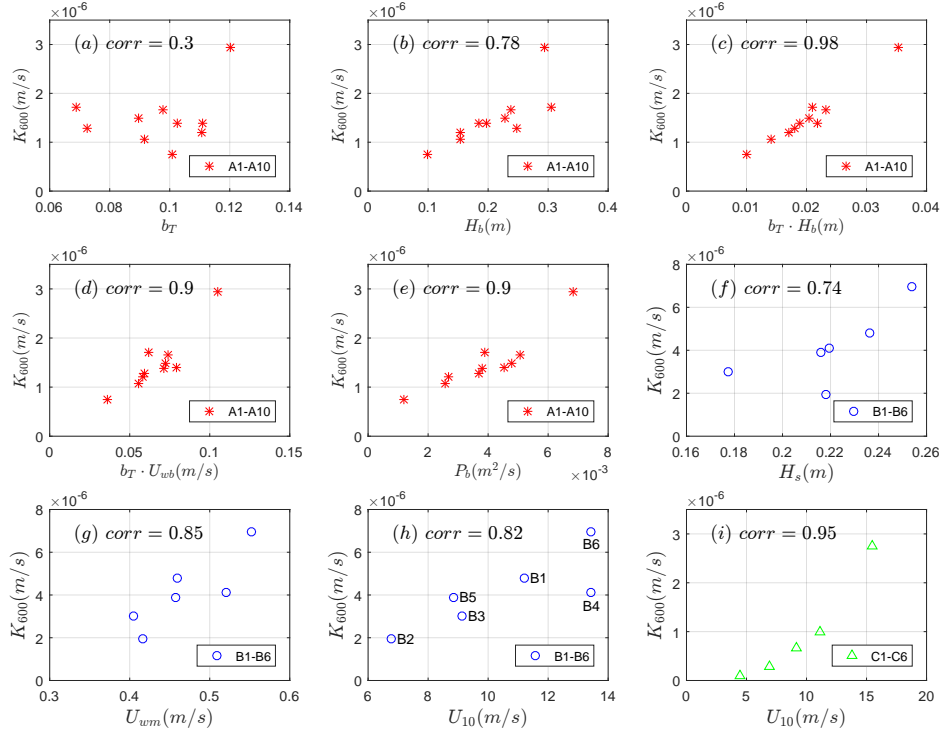
Figure 2. CO_2 gas transfer velocity of monochromatic wave experiments versus (a) wave breaking probability, (b) mean wave height of breakers, (c) product of breaking probability and mean wave height of breakers, (d) product of breaking probability and mean wave orbital velocity of breakers, (e) mean energy loss of breakers upstream nearest the sampling tubing per unit of time. CO_2 transfer velocity of coupled wave experiments versus (f) significant wave height, (g) mean wave orbital velocity, (h) 10-meter wind speed. CO_2 gas transfer velocity of wind wave experiments versus (i) 10-meter wind speed

and 10-meter wind speed (figure 2(h)). The superimposed wind not only adjusts the wave breaking (e.g. breaking probability) but also ripples the flat surface of non-breaking mechanically-generated waves which implies the energy transfer from wind to waves and hence promoted gas exchange velocity. As a result, statistical parameters H_s and U_{wm} which are based on all waves rather than breaking wave parameters (H_b or U_{wb}) are in good correlation with K_{600}. The wind speed is also well correlated with the K_{600} (figure 2(h)), but experiments with similar U_{10} can lead to different K_{600} (e.g. B4 and B6 in panel(h)), which demonstrates the uncertainties in the parameterization with wind speed alone.

In wind wave experiments (C1-C6), K_{600} has a quadratic relation with wind speed (figure 2(i)). Similar high correlations are also found between K_{600} and wave parameters such as wave height and orbital velocity because waves at a fixed fetch grow with the increased wind forcing. From the figure 2(h) and (i), wind speed is a good parameter to describe gas exchange within each kind of experiment but can not collapse all the data sets.

From the correlation analysis, CO_2 exchange velocity is determined by water-side turbulence which is related with breaking probability, turbulence originated from each breaking event and turbulence of non-breaking waves affected by wind. The wind plays an indirect role by transferring energy into waves and direct but insignificant role by creating turbulence beyond water surface. The parameterization of CO_2 exchange velocity should be able to unify all data sets and physically reasonable. First, considering that K_{600} is of a different order for open ocean (i.e. to avoid the dependence on the dimensional wave parameters), it is scaled by the mean orbital velocity (U_{wm}) of waves through (5).

$$\tilde{K} = \frac{K_{600}}{U_{wm}}, \tag{5}$$

where $\tilde{K}$ is now a non-dimensional gas transfer velocity and directly related with waves. Meanwhile, in view of the good correlation of wave parameters with K_{600} in figure 2, wave Reynolds numbers are used to denote the turbulent degree in water with different parameters. R_{HW} in equation (6) is the multiplication of breaking wave height and orbital velocity and then divided by ν_w, which is the viscosity of water. R_{HW} highlight the effect of breaking waves based on the analysis of experiments A1-A10 in figure 2(a) to (e). R_M in equation (7), on the other hand, consists of significant wave height, mean orbital velocity and ν_w. R_M is developed by considering the statistical parameters based on all waves from the analysis of B1-B6 in figure 2(f) to (h).

$$R_{HW} = \frac{H_b \cdot U_{wb}}{\nu_w}, \tag{6}$$

$$R_M = \frac{H_s \cdot U_{wm}}{\nu_w}, \tag{7}$$

Wind speed is also scaled as in equation (8), which is also introduced in Lenain and Melville (2017).

$$\tilde{U} = \frac{U_*}{\sqrt{g \cdot H_s}}, \tag{8}$$

where $\tilde{U}$ is non-dimensional wind speed, U_* is the wind friction velocity, g is gravitational acceleration. It should be noted that $\sqrt{g \cdot H_s}$ is proportional to wave peak phase velocity C_p in fetch-limited condition. Thus, $\tilde{U}$ has the meaning of the inverse of wave age.

In figure 3(a), b_T alone obviously can not unify the results of all experiments. In figure 3(b), R_{HW} performs better but the disparity between data sets is still evident. In figure 3(c), the product of b_T and R_{HW} is used which signifies the importance of both wave breaking probability and wave breaking related turbulence, and the correlation is improved. As mentioned above, wind also transfers energy into non-breaking waves and creates turbulence at air-side. Considering the indirect role of wind forcing, the scaled
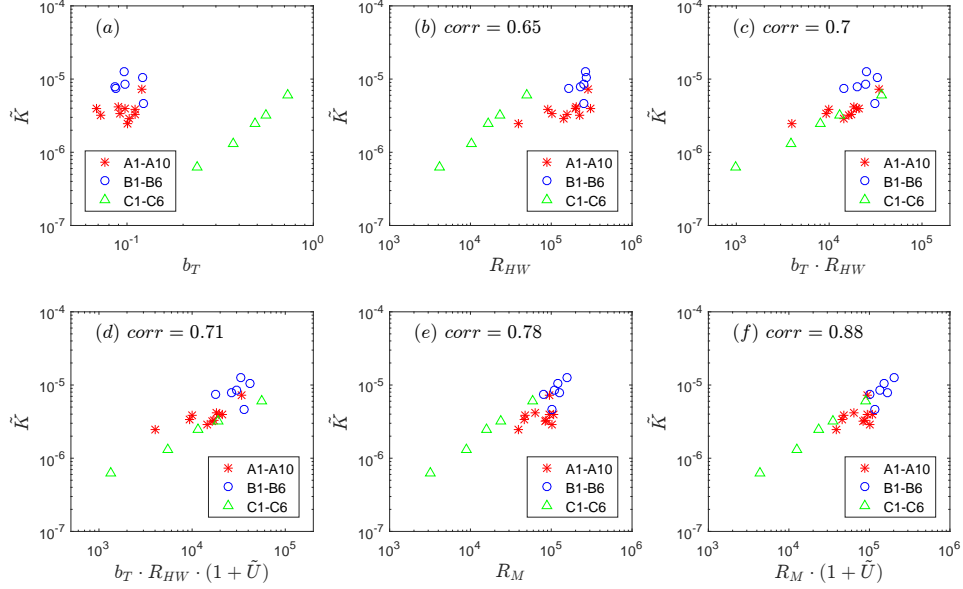
Figure 3. Non-dimensional CO_2 gas transfer velocity versus (a) wave breaking probability, (b) Reynolds number (R_{HW}), (c) product of breaking probability and Reynolds number (R_{HW}), (d) product of breaking probability, Reynolds number (R_{HW}) and scaled wind speed, (e) Reynolds number (R_M), (f) product of Reynolds number (R_M) and scaled wind speed

wind speed is multiplied as an enhancement factor as $(1+\tilde{U})$ in figure 3(d). When wind forcing approaches zero, the results converge to the no-wind (mechanically generated) conditions. The correlation is slightly improved and the parameterization is physically more reasonable. In figure 3(e) and (f), R_M alone performs well in unifying the data sets and the correlation coefficient is further improved from 78% to 88% by multiplying with $(1+\tilde{U})$. It should also be mentioned that wind speed alone is unable to reconcile the results of B1-B6 and C1-C6.

The whole expression from figure 3(d) is then written as equation (9):

$$\tilde{K} = \alpha \cdot (b_T \cdot R_{HW} \cdot (1+\tilde{U}))^\beta, \tag{9}$$

where the fitting parameters α and β are $4.49 \cdot 10^{-9}$ and 0.70, respectively. The resulted coefficient of determination is 76%. The expression from figure 3(f) is written in equation (10):

$$\tilde{K} = \alpha \cdot (R_M \cdot (1+\tilde{U}))^\beta, \tag{10}$$

Where the fitting parameters α and β are $1.98 \cdot 10^{-9}$ and 0.69, respectively, with resulted coefficient of determination to be 82%.

4 Discussion and Conclusions

Considering the fact that water-side dynamic processes have direct impact on CO_2 gas exchange, we scale k_{600} with the mean wave orbital velocity rather than wind speed in equation (5). The orbital velocity is chosen also because water mass moves along with orbital motion. Equation (9) is established to highlight the effect of wave breaking for CO_2 gas exchange at sea - it is responsible both for production of bubbles and excessive amount of turbulence (Agrawal et al., 1992). b_T and R_{HW} denote the rate and cor-

responding turbulent degree of wave breaking events. Equation (10) uses the Reynolds number R_M that is statistically based on all waves, in order to denote the overall wave-related turbulence. $\tilde{U}$ is proportional to the inverse of wave age, which represents the momentum transfer efficiency from wind to waves. The term $(1+\tilde{U})$ not only improves the correlation in our analysis, but also denotes the indirect role of wind forcing to the gas exchange.

Similar form of Reynolds numbers have been used to denote wind-sea turbulence, such as $R_{AW} = \frac{U_* H_s}{\nu_w}$ and $R_{BW} = \frac{U_*^2}{\nu_w \omega_p}$ in Zhao and Xie (2010) and Brumer et al. (2017), where ω_p is peak frequency of ocean waves. The wind forcing in R_{AW} and R_{BW} shares equal or higher significance compared with wave parameters. As mentioned above, the waves and wave breaking rather than wind directly facilitate CO_2 gas exchange. In monochromatic wave experiments (A1-A10), the waves evolve to unsteady state and eventually break without wind ($U_* = 0$), which breaking still promotes the gas transfer rate. Therefore, the wave orbital velocity replaces the wind speed U_* in our parameterization so that the K_{CO_2} in equation (9) and (10) mainly depend on the features of waves. Nonetheless, our formulae need to be further validated by field data.

In the experiments, the measured CO_2 gas exchange velocity is less than other reported values from laboratory(e.g. Ocampo-Torres et al., 1994). The reason is that the whole water in wave tank is not always circulated and mixed once the measurements start. The local CO_2 concentration change with time is also affected by water upstream due to stokes drift. Thus, the $\frac{\partial C_g}{\partial t}$ in equation (2) is changed to be $\frac{dC_g}{dt}$. The procedure of our experiments serves the purpose to simulate the gas exchange affected by deep water waves at ocean surface, where the mixing depends on the wind-sea state. In laboratory, mixing the water provides homogeneous CO_2 concentration, but it is difficult to evaluate the impact of extra turbulence and its interaction with wave field.

Finally, we summarize the main findings in present work. The breaking probability together with wave height or orbital velocity, energy loss of breakers and wind speed are found to be well correlated with the gas exchange velocity. To parameterize the dependence, formulae are built based on wave properties directly. Mean wave orbital velocity is used to scale CO_2 transfer rate. The breaking probability and wave Reynolds numbers are used as the dominant term to represent wave effect. The scaled wind speed is employed as an enhancement factor.

Acknowledgments

References

Agrawal, Y., Terray, E., Donelan, M., Hwang, P., Williams, A., Drennan, W. M., ... Krtaigorodskii, S. (1992). Enhanced dissipation of kinetic energy beneath surface waves. *Nature*, *359*(6392), 219–220.

Babanin, A., Waseda, T., Kinoshita, T., & Toffoli, A. (2011). Wave breaking in directional fields. *Journal of Physical Oceanography*, *41*(1), 145–156.

Babanin, A. V., Chalikov, D., Young, I., & Savelyev, I. (2007). Predicting the breaking onset of surface water waves. *Geophysical research letters*, *34*(7).

Babanin, A. V., Chalikov, D., Young, I., & Savelyev, I. (2010). Numerical and laboratory investigation of breaking of steep two-dimensional waves in deep water. *Journal of Fluid Mechanics*, *644*, 433–463.

Banner, M. L., Babanin, A. V., & Young, I. R. (2000). Breaking probability for dominant waves on the sea surface. *Journal of Physical Oceanography*, *30*(12), 3145–3160.

Brumer, S. E., Zappa, C. J., Blomquist, B. W., Fairall, C. W., Cifuentes-Lorenzen, A., Edson, J. B., . . . Huebert, B. J. (2017). Wave-related reynolds number parameterizations of co2 and dms transfer velocities. *Geophysical Research Letters*, *44*(19), 9865–9875.

Fairall, C., Yang, M., Bariteau, L., Edson, J., Helmig, D., McGillis, W., . . . Blomquist, B. (2011). Implementation of the coupled ocean-atmosphere response experiment flux algorithm with co2, dimethyl sulfide, and o3. *Journal of Geophysical Research: Oceans*, *116*(C4).

Fortescue, G., & Pearson, J. (1967). On gas absorption into a turbulent liquid. *Chemical Engineering Science*, *22*(9), 1163–1176.

Galchenko, A., Babanin, A. V., Chalikov, D., Young, I., & Haus, B. K. (2012). Influence of wind forcing on modulation and breaking of one-dimensional deep-water wave groups. *Journal of Physical Oceanography*, *42*(6), 928–939.

Jähne, B., Münnich, K. O., Bösinger, R., Dutzi, A., Huber, W., & Libner, P. (1987). On the parameters influencing air-water gas exchange. *Journal of Geophysical Research: Oceans*, *92*(C2), 1937–1949.

Lamont, J. C., & Scott, D. (1970). An eddy cell model of mass transfer into the surface of a turbulent liquid. *AIChE Journal*, *16*(4), 513–519.

Lenain, L., & Melville, W. K. (2017). Measurements of the directional spectrum across the equilibrium saturation ranges of wind-generated surface waves. *Journal of Physical Oceanography*, *47*(8), 2123–2138.

Liang, J.-H., Deutsch, C., McWilliams, J. C., Baschek, B., Sullivan, P. P., & Chiba, D. (2013). Parameterizing bubble-mediated air-sea gas exchange and its effect on ocean ventilation. *Global Biogeochemical Cycles*, *27*(3), 894–905.

Melville, W. K. (1996). The role of surface-wave breaking in air-sea interaction. *Annual review of fluid mechanics*, *28*(1), 279–321.

Ocampo-Torres, F., Donelan, M., Merzi, N., & Jia, F. (1994). Laboratory measurements of mass transfer of carbon dioxide and water vapour for smooth and rough flow conditions. *Tellus B: Chemical and Physical Meteorology*, *46*(1), 16–32.

Pachauri, R. K., Allen, M. R., Barros, V. R., Broome, J., Cramer, W., Christ, R., . . . others (2014). *Climate change 2014: synthesis report. contribution of working groups i, ii and iii to the fifth assessment report of the intergovernmental panel on climate change.* Ipcc.

Thomson, J., Schwendeman, M. S., Zippel, S. F., Moghimi, S., Gemmrich, J., & Rogers, W. E. (2016). Wave-breaking turbulence in the ocean surface layer. *Journal of Physical Oceanography*, *46*(6), 1857–1870.

Wanninkhof, R., Asher, W. E., Ho, D. T., Sweeney, C., & McGillis, W. R. (2009). Advances in quantifying air-sea gas exchange and environmental forcing.

Woolf, D. K. (1997). Bubbles and their role in gas exchange. *The sea surface and global change*.

Zappa, C. J., Asher, W., Jessup, A., Klinke, J., & Long, S. (2004). Microbreaking and the enhancement of air-water transfer velocity. *Journal of Geophysical Research: Oceans*, *109*(C8).

Zhao, D., Toba, Y., Suzuki, Y., & Komori, S. (2003). Effect of wind waves on air–sea gas exchange: proposal of an overall co2 transfer velocity formula as a function of breaking-wave parameter. *Tellus B*, *55*(2), 478–487.

Zhao, D., & Xie, L. (2010). A practical bi-parameter formula of gas transfer velocity depending on wave states. *Journal of oceanography*, *66*(5), 663–671.